Nanoscale Res Lett (2010) 5:1–6
DOI 10.1007/s11671-009-9433-4

NANO EXPRESS

Magnetic Properties of FePt Nanoparticles Prepared by a Micellar Method

Y. Gao · X. W. Zhang · Z. G. Yin · S. Qu · J. B. You · N. F. Chen

Received: 30 July 2009 / Accepted: 1 September 2009 / Published online: 16 September 2009

Abstract FePt nanoparticles with average size of 9 nm were synthesized using a diblock polymer micellar method combined with plasma treatment. To prevent from oxidation under ambient conditions, immediately after plasma treatment, the FePt nanoparticle arrays were in situ transferred into the film-growth chamber where they were covered by an SiO_2 overlayer. A nearly complete transformation of $L1_0$ FePt was achieved for samples annealed at temperatures above 700 °C. The well control on the FePt stoichiometry and avoidance from surface oxidation largely enhanced the coercivity, and a value as high as 10 kOe was obtained in this study. An evaluation of magnetic interactions was made using the so-called isothermal remanence (IRM) and dc-demagnetization (DCD) remanence curves and Kelly–Henkel plots (ΔM measurement). The ΔM measurement reveals that the resultant FePt nanoparticles exhibit a rather weak interparticle dipolar coupling, and the absence of interparticle exchange interaction suggests no significant particle agglomeration occurred during the post-annealing. Additionally, a slight parallel magnetic anisotropy was also observed. The results indicate the micellar method has a high potential in preparing FePt nanoparticle arrays used for ultrahigh density recording media.

Keywords FePt nanoparticles · Reverse micelles · Self-assembly · Interparticle exchange coupling · Magnetic recording

Y. Gao · X. W. Zhang (✉) · Z. G. Yin · S. Qu · J. B. You · N. F. Chen
Key Lab of Semiconductor Materials Science, Institute of Semiconductors, CAS, Beijing 100083, People's Republic of China
e-mail: xwzhang@semi.ac.cn

Introduction

Patterned single-domain magnetic nanoparticles, with each one carrying one bit of information, have been considered as one of the best candidates for future ultrahigh density recording media [1]. In such a scheme, enhancing the storage density needs a reduction in nanoparticle diameter and spacing, hence materials with high magnetocrystalline anisotropy constant K_u are required to enhance the thermal stability. Face-centered-tetragonal (FCT) $L1_0$ phase FePt has been receiving considerable attention due to its high K_u (7×10^7 ergs/cc) [2], a value that is of the largest among the known hard magnetic materials. Theoretical calculations indicate that FePt particles as small as 3 nm are sufficiently stable and satisfy the requirements of permanent data storage [3]. Great efforts have been devoted to search a convenient way for synthesizing $L1_0$ phase FePt nanoparticle arrays. Traditional physical deposition techniques have difficulties in controlling the particle size and morphology due to the random nucleation during the initial growth stage. A colloidal-chemical route, since the seminal work of Sun et al. [4], has proven to be a powerful way to synthesize FePt nanoparticles with uniform size and well-defined interparticle spacing. The as-prepared nanoparticles by colloidal technique possess atomically disordered face-centered-cubic (FCC) structure and are superparamagnetic in nature. Thermal annealing with temperature higher than 500 °C is usually needed to induce the FCC–FCT transition. During the post-annealing process, however, the agglomeration of particles due to the rather small interparticle spacing can result in a drastic increase of particle size, as well as a very strong interparticle exchange coupling [5, 6]. In addition, the ligand shell is expected to influence the magnetic properties and can be converted to

a carbonaceous coating around particles during the post-annealing process [7].

A micellar method has been adopted by Ethirajan et al. [8] and Qu et al. [9] to overcome these obstacles. The preparation of metal nanoparticle arrays by this method is based on the self-assembly of suitable diblock copolymers [10]. When the diblock copolymers are dissolved into an apolar solvent, they form spherical reverse micelles. The cores of such reverse micelles can be loaded with metal salts. The reverse micelles self-organize into hexagonally ordered arrays when a monolayer of them covers a smooth substrate. Properly removing the polymer matrix, the resultant metal nanoparticles hold the initial pattern of the reverse micelles. This method has a high flexibility in controlling the particle size, interparticle spacing, and composition. The size distributions of the obtained nanoparticles are comparable to or even better than those of the colloidal nanoparticles [11]. Although the micellar method has been demonstrated successful in synthesizing FePt nanoparticle arrays [8, 9], few works are available on their magnetic properties. The reported coercivity of FePt nanoparticles synthesized by the micellar method is merely 1500 Oe [8], which is far from being ideal for a recording medium.

Herein, we present a detailed investigation on the structural and magnetic properties of FePt nanoparticles fabricated by the micellar method. Based on previous works [9, 12], the ordered FePt nanoparticle arrays with ideal 1:1 stoichiometry were successfully synthesized. Post-annealing treatments were employed to induce the formation of $L1_0$ phase FePt nanoparticles. A high value (10 kOe) of the coercivity (H_C) has been achieved for the sample annealed at temperatures above 700 °C. Moreover, the absence of interparticle exchange coupling suggests no significant particle agglomeration occurred during the post-annealing, which leads to lower media noise.

Experiment Details

The preparation of FePt nanoparticles was based on the self-assembly of poly(styrene)–poly(4-vinylpyridine), i.e., PS–P4VP, into reverse micelles in toluene. H_2PtCl_6 and $FeCl_3$ were added into the micellar solution and then micelles loaded with metal salts were deposited on silicon substrates by a dip-coating process. Details on the process have been published elsewhere [12]. In order to remove the polymer matrix and to finally reduce the nanoparticles into metallic states, the as-coated samples were subsequently subjected to oxygen and hydrogen plasma treatment for 30 min (150 Pa, 100 W) within a home-made radio frequency (RF) plasma system. Immediately after the plasma treatments, the samples were in situ transferred into the film-deposition chamber where they were covered by a 10-nm-thick SiO_2 layer using RF magnetron sputtering. Coating the SiO_2 layer is to protect the FePt nanoparticles from oxidation in ambient, as well as to prevent them from agglomeration during annealing. The procedure from dip-coating to SiO_2 deposition was repeated for 10 times. Finally, vacuum annealing treatments were performed to drive the FCC–FCT transition.

Surface morphologies of the monolayer samples were characterized by a NT-MDT Solver P47 atomic force microscopy (AFM) in a semi-contact mode. For the X-ray diffraction (XRD) measurements in a θ–2θ mode, a Panalytical X'Pert-MPD Pro diffractometer with a Cu K_α X-ray source was used. Transmission electron microscopy (TEM) analysis was carried out by a JEM-2010 microscope. Room-temperature magnetic hysteresis loops and ΔM curves were measured by a model MicroMag-2900 alternating gradient magnetometer (AGM).

Results and Discussion

The closely packed reverse micelles loaded with Fe and Pt salts exhibit a quasi-hexagonal pattern, as shown in Fig. 1a. The micelles are very uniform in size with inter-micelle distance of about 40 nm. Figure 1b shows the corresponding AFM topography image of the FePt nanoparticles after the plasma treatment, obviously, the lateral order of the resulting FePt nanoparticles is conserved. Local order is reasonably good as proven by the autocorrelation image in the inset of Fig. 1b. This indicates that the carefully designed etching process has little influence upon the order of the resulting FePt nanoparticle arrays. The average height of the metal–salt-loaded micelles and FePt nanoparticles is determined to be about 15.0 and 9.0 nm, respectively. The size distributions of the micelles and FePt nanoparticles extracted from Fig. 1a and b exhibit Gaussian characteristics, as shown in Fig. 1c and d. The standard deviations of the size distributions are 5 and 6% for the micelles and FePt nanoparticles, respectively, indicating that this block copolymer template method is a very effective means of generating uniformly sized FePt nanoparticles.

It is very important to insure the complete removal of the PS–P4VP matrix by plasma treatment, otherwise the residuals would form carbonaceous contamination during post-annealing, influencing the magnetic behaviors of FePt nanoparticles. The X-ray electron spectroscopy (XPS) signals from C 1*s* and N 1*s* were used to determine whether the matrix is absent [9]. The results show that the polymer matrix can be completely removed through a 30 min oxygen plasma treatment. After the oxygen plasma treatment, Fe and Pt atoms are in highly oxidized state [9].

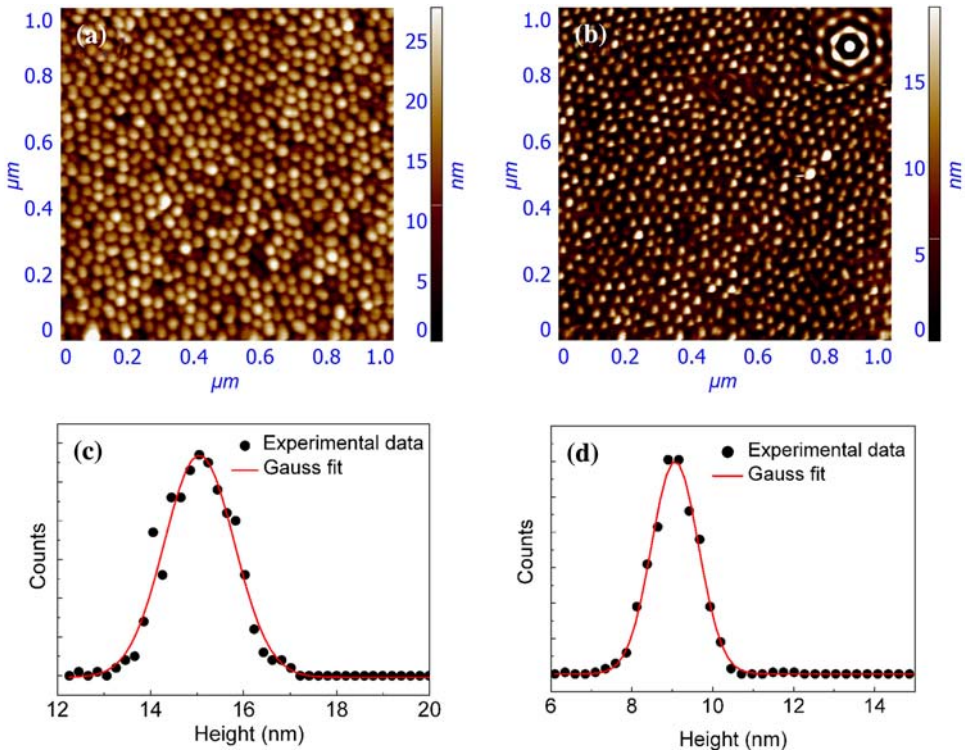

Fig. 1 AFM topography images of **a** the as-coated PS–PVP micelles loaded with H_2PtCl_6 and $FeCl_3$, and **b** the FePt nanoparticles arrays obtained after plasma treatment (the inset is the corresponding autocorrelation function). The corresponding size distributions are shown in (**c**) and (**d**)

Undergone a subsequent hydrogen plasma treatment (30 min, 100 W), the Fe and Pt atoms were reduced to a metallic state. Rutherford backscattering spectroscopy (RBS) measurements reveal that the plasma treatment adopted here produces scarcely any loss of the metal atoms [12]. The synthesis of carbon-contamination free, metallic FePt nanoparticles favors their applications in ultrahigh density data recording.

To verify the crystalline structure of FePt nanoparticles, the XRD experiment was performed on a monolayer FePt nanoparticles synthesized on Si substrates. However, the amount of nanoparticles on substrates was not enough to obtain an adequate signal-to-noise ratio, and only an ignorable signal was obtained even for the annealing sample. Therefore, TEM images, as shown in Fig. 2, were taken to analyze mircostructure of the 700 °C annealed monolayer nanoparticles covered by a SiO_2 overlayer. The FePt nanoparticles consists mainly of single-domain particles with some small amount of twinned particles, and the electron diffraction pattern shown as inset to the figure confirms that the $L1_0$ phase FePt alloy nanoparticles were formed.

To improve the intensities of XRD and magnetic signal, the procedure from dip-coating to SiO_2 deposition was repeated for 10 times. Figure 3 shows the 2θ–θ XRD patterns of the samples annealed at different temperatures (500–750 °C) with holding time of 60 min. From these patterns, we found: (i) only a very weak and broad FePt (111) peak was visible for the sample annealed at 500 °C;

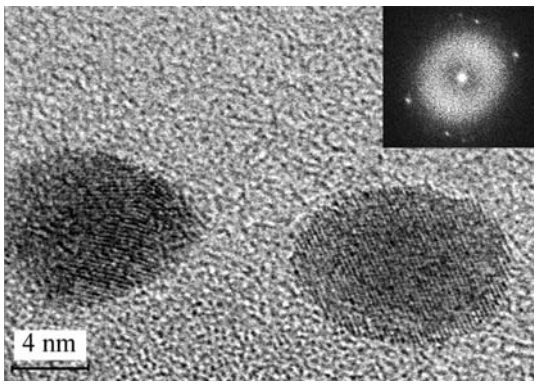

Fig. 2 TEM image of the monolayer FePt nanoparticle array covered by a SiO_2 overlayer after 700 °C annealing for 60 min, and the corresponding electron diffraction pattern is shown as inset

(ii) as annealing temperature, T_a, went up to 600 °C, both (001) and (110) reflections were resolved and their intensities enhanced with increasing T_a; (iii) the splitting of {002} into (002) and (200) variants occurred at T_a higher than 600 °C. Clearly, the 500 °C annealed sample consists mainly of the chemically disordered FCC phase, since (001) and (110) reflections are absent in FCC FePt due to structure extinction. The formation of FCT FePt involves a lattice distortion [13], making the extinction conditions unsatisfied. As a result, (001) and (110) reflections, as well as the splitting of {002}, appear in FCT FePt. Thus, we can conclude based on the XRD patterns that the FCC-FCT transition occurs at about 600 °C, and the ordered volume

fraction grows up with increasing T_a. The ordering parameter S, which is a measure of the volume fraction of the FCT phase, is given by [14]

$$S^2 \equiv \frac{1-(c/a)}{1-(c/a)_{S_f}} \quad (1)$$

where (c/a) is the experimental axial ratio for the partially ordered phase, and $(c/a)_{S_f}$ is the theoretical one for the chemically ordered FCT phase. $S = 1$ means the FePt nanoparticles are fully in the ordered FCT phase. Here $(c/a)_{S_f}$ was determined to be 0.96 according to Ref. [15]. The axial ratio of the sample annealed at $T_a = 700$ °C can be evaluated from the XRD peaks in Fig. 3c. Accordingly, the value of S obtained by Eq. 1 is 0.91, very close to 1. It means that most of the FePt nanoparticles have transformed to the chemically ordered FCT phase after 700 °C annealing for 60 min.

In-plane magnetic hysteresis (M-H) loops were measured at room temperature by AGM using an 18 kOe saturating field. Figure 4a shows the M-H curves of the samples annealed at different temperatures for 60 min. Because the maximum applied field of the used AGM equipment is limited to 18 kOe, some of hysteresis loops in Fig. 4 are not completely saturated. However, the symmetric and the nearly closed loops imply that the value of 18 kOe is quite close to that of the saturation magnetization field. The 500 °C annealed sample is magnetically soft. At $T_a = 600$ °C, the coercivity exhibits a significant increase, indicating the occurrence of FCC–FCT transition, consistent with the results of XRD. Further increasing T_a results in a dramatic rise in H_C, and a value of 10 kOe can be achieved when T_a exceeds 700 °C. The dependence of the coercivity on T_a is shown in the inset of Fig. 4a. Here we note that even at $T_a = 700$ °C, a holding time of 60 min is needed to complete the FCC–FCT transformation. As

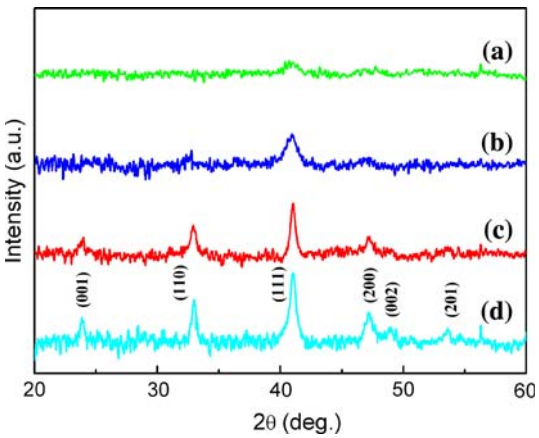

Fig. 3 X-ray diffraction (θ–2θ scan) patterns of the FePt samples annealed at (a) 500, (b) 600, (c) 700, and (d) 750 °C for 60 min in vacuum

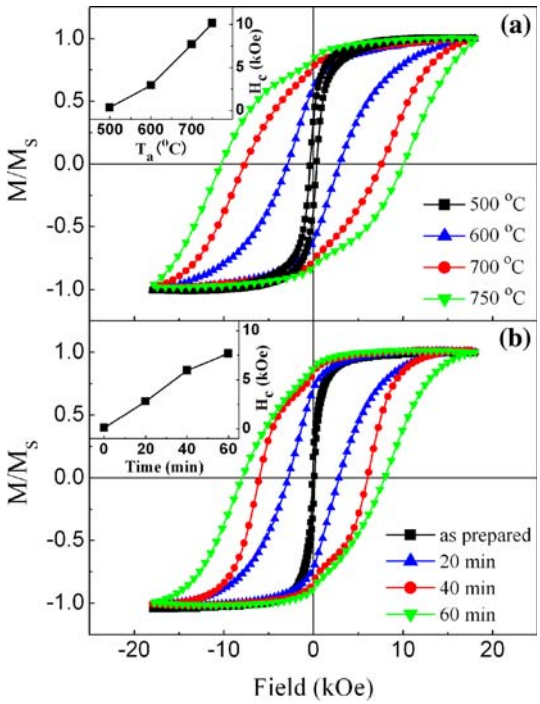

Fig. 4 In-plane M-H loops for the samples **a** annealed at various temperatures with holding time of 60 min, and **b** annealed at 700 °C with different holding times

clearly shown in Fig. 4b, the as-prepared sample exhibits a very soft nature, with a coercivity of ~100 Oe. This finite value of H_C may be attributed to a rather small fraction of FCT FePt resulting from structural nonuniformity. A significant rising of H_C with increasing annealing time was observed until it reaches to 60 min, as demonstrated in the inset of Fig. 4b. Further, increasing the annealing time does not help enhancing the coercivity, and actually the ordering parameter S value of 0.91 is close to 1 for the sample annealed at 700 °C for 60 min. These results imply that the most of the FePt nanoparticles have transformed to the FCT phase.

A suitable high H_C is technologically important for high-density recording media. The coercivity of ~10 kOe we obtained is much higher than 1.5 kOe reported in Ref. [8] and 2.2 kOe in Ref. [16]. However, it is still less than the theoretical coercivity value of 9 nm FCT FePt nanoparticles. For assembly of randomly distributed single-domain particles with uniaxial anisotropy, by taking the theoretically saturation magnetization (M_S) and magnetocrystalline anisotropy values, a coercivity of 30 kOe is calculated for fully ordered 9 nm $Fe_{50}Pt_{50}$ particles [17]. Generally, stoichiometry deviation from 1:1 [16, 18], surface oxidization [7], the multidomain effect, and the formation of a silicide structure [19] may be possible explanations for the smaller H_C as compared with the calculated one. In order to obtain $L1_0$ phase, the alloy must

have a composition between 33 and 55 at.%, as determined from the Fe–Pt phase diagram [20]. It is difficult for nanoparticle with Fe/Pt ratio significantly deviating from 1:1 to transform into the hard magnetic phase upon annealing [18]. In a recent work [12], we have investigated the composition deviation of FePt nanoparticles from the nominal Fe:Pt molar ratio of the precursors. Based on the research, a better control over the particle stoichiometry has been achieved. Furthermore, in this work, to avoid the surface oxidization of FePt nanoparticles, the FePt samples were in situ transferred into the film-deposition chamber and covered by an SiO_2 overlayer after hydrogen plasma treatment. Therefore, in the present work, the possibilities of stoichiometry deviation and surface oxidization can be excluded, and the multidomain effect and the formation of a silicide structure may be responsible for the smaller H_C.

Here we note that nearly identical in-plane and out-of-plane loops were observed for the sample annealed at 500 °C, implying a randomly distribution of easy magnetization axes. As the annealing temperature increased to 600 °C, both the coercivity and remanence of the in-plane loop are somewhat larger than those of the out-of-plane loop (Fig. 5), indicating the occurrence of slight parallel magnetic anisotropy. It is notable that a major challenge now is to produce arrays of FePt nanoparticles with oriented magnetic easy axes, which is extremely important from the viewpoint of practical use [21]. However, although tremendous attention [1, 14, 21, 22] has been paid on this issue, a general strategy is still far from being achieved. A possible explanation for the slight parallel anisotropy observed here is related to the thermal stress caused by annealing treatment. During the annealing process, the thermal stress along the sample normal satisfies $\sigma_Z \approx 0$, while considerably huge in-plane stress can be induced due to the rather large thermal expansion coefficient (10.5×10^{-6} K^{-1}) of FePt [23], as compared with that (2.5×10^{-6} K^{-1}) of the Si substrate. The FCC–FCT transformation involves a lattice distortion with the c lattice parameter contracts approximately 2% [3]. The c-axis of FePt prefers to align in the plane, which may greatly alleviate the thermal stress. Further research is underway to clarify the origin of the preferential in-plane c-axis alignment and the resultant parallel anisotropy.

In order to explore the interparticle magnetic interactions of the FePt nanoparticles, we have measured the isothermal remanent magnetization (IRM) and DC demagnetized (DCD) magnetization as functions of the applied magnetic field at room temperature for the sample annealed at 750 °C. The results are shown in Fig. 6a. The IRM measurement starts from the demagnetized state. A magnetic field is applied on the surface, then it is switched off and the remanent magnetization is measured. Such a measurement was performed again as the magnetic field increased by ΔH. This routine was repeated constantly until the saturated remanence was reached. Plotting the measured remanence data as a function of the magnetic field, an IRM curve is obtained. By comparison, the DCD measurement starts from the saturated state. A routine similar to the IRM measurement is used, while in this case the external field is applied in the opposite direction (negative fields). ΔM is defined as $M_d - (1 - 2M_r)$, where M_d and M_r are the normalized DC remanence and isothermal remanence, respectively [24]. Generally speaking, for non-interactional single-domain particles, $\Delta M = 0$; a positive ΔM indicates interparticle exchange coupling while a negative value suggests a long-range dipolar interaction [25]. Figure 6b shows the ΔM curve calculated

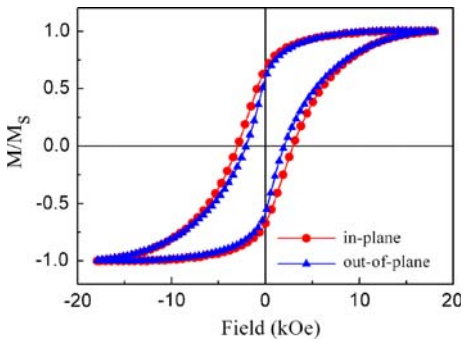

Fig. 5 In-plane and out-of-plane M-H loops for the sample annealed at 600 °C for 60 min

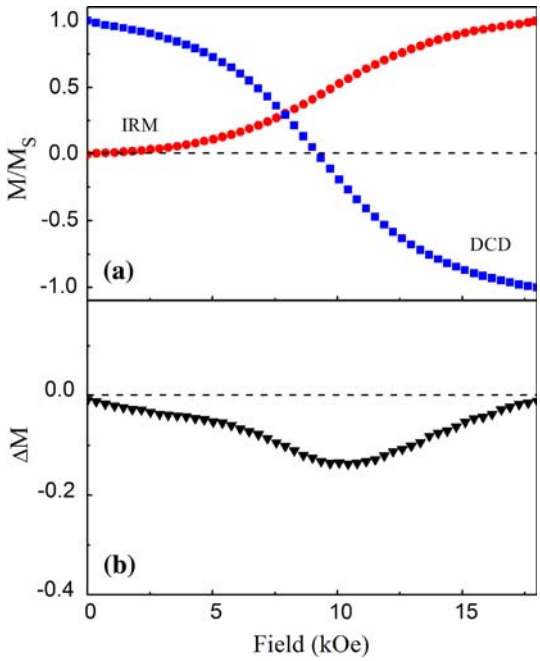

Fig. 6 a IRM and DCD curves at room temperature for the FePt sample annealed at 750 °C; **b** ΔM curve obtained from the IRM and DCD data

according to the IRM and DCD data illustrated in Fig. 6a. An overall small negative ΔM was observed, indicating a weak dipolar interaction between the nanoparticles. The absence of interparticle exchange coupling confirmed that most of the particles were well-separated during the post-annealing without any agglomeration [25]. Both the large interparticle distance and the SiO_2 layers help isolating the nanoparticles. The results indicate the micellar method has a high potential in preparing FePt nanoparticle arrays used for ultrahigh density recording media.

Conclusions

In conclusion, we have prepared FePt nanoparticles on Si substrate by a micellar method, with small particle size (9.0 nm) and a very narrow size distribution. The as-prepared samples by dip-coating were exposed to plasma to completely remove the polymer matrix and reduce the atoms into metallic state. Post-annealing was performed to induce the formation of chemically ordered FCT $L1_0$ phase. An ordering parameter higher than 0.9 was achieved for the samples annealed at 700 °C or above for 60 min. By better control on the FePt stoichiometry and avoidance from surface oxidation, a large in-plane coercivity of $\sim$10 kOe was obtained in this study. A slight parallel magnetic anisotropy was also observed. In addition, no evident interparticle exchange coupling was observed for the FePt particles, suggesting no significant agglomeration occurred during the post-annealing. The FePt nanoparticles prepared by micellar method have a high potential for use in magnetic data recording.

Acknowledgments This work was financially supported by the National High-tech R&D Programme of China under Grant No 2006AA03Z306, and the National Natural Science Foundation of China under Grant No 50601025 and 60806044.

References

1. M. Chen, J. Kim, J.P. Liu, H. Fan, S. Sun, J. Am. Chem. Soc. **128**, 7132 (2006)
2. D. Weller, A. Moser, IEEE Trans. Magn. **35**, 4423 (1999)
3. H.L. Nguyen, L.E.M. Howard, S.R. Giblin, B.K. Tanner, I. Terry, A.K. Hughes, I.M. Ross, A. Serres, H. Bürckstümmer, J.S.O. Evans, J. Mater. Chem. **15**, 5136 (2005)
4. S.H. Sun, C.B. Murray, D. Weller, L. Folks, A. Moser, Science **287**, 1989 (2000)
5. H. Zeng, M.L. Yan, N. Powers, D.J. Sellmyer, Appl. Phys. Lett. **80**, 2350 (2002)
6. Z.R. Dai, S.H. Sun, Z.L. Wang, Nano Lett. **1**, 443 (2001)
7. S. Sanders, M.F. Toney, T. Thomason, J.U. Thiele, B.D. Terris, S.H. Sun, C.B. Murray, J. Appl. Phys. **93**, 7343 (2003)
8. A. Ethirajan, U. Wiedwald, H.G. Boyen, B. Kern, L.Y. Han, A. Klimmer, F. Weigl, G. Kastle, P. Ziemann, K. Fauth, J. Cai, R.J. Behm, A. Romanyuk, P. Oelhafen, P. Walther, J. Biskupek, U. Kaiser, Adv. Mater. **19**, 406 (2007)
9. S. Qu, X.W. Zhang, Z.G. Yin, J.B. You, N.F. Chen, Chin. Phys. Lett. **24**, 3520 (2007)
10. J.P. Spatz, S. Mössmer, C. Hartmann, M. Möller, T. Herzog, M. Krieger, H.G. Boyen, P. Ziemann, B. Kabius, Langmuir **16**, 407 (2000)
11. G. Kästle, H.G. Boyen, F. Weigl, G. Lengl, T. Herzog, P. Ziemann, S. Riethmüller, O. Mayer, C. Hartmann, J.P. Spatz, M. Möller, M. Ozawa, F. Banhart, M.G. Garnier, P. Oelhafen, Adv. Funct. Mater. **13**, 853 (2003)
12. S. Qu, X.W. Zhang, Y. Gao, J.B. You, Y.M. Fan, Z.G. Yin, N.F. Chen, Nanotechnology **19**, 135704 (2008)
13. S. Kang, Z. Jia, S. Shi, D.E. Nikles, J.W. Harrell, Appl. Phys. Lett. **86**, 062503 (2005)
14. B.W. Robarts, Acta Metall. **2**, 597 (1954)
15. S. Iwasaki, IEEE Trans. Magn. **20**, 657 (1984)
16. H.B. Wang, M.J. Zhou, F.J. Yang, J. Wang, Y. Jiang, Y. Wang, H. Wang, Q. Li, Chem. Mater. **21**, 404 (2009)
17. H. Pfeiffer, Phys. Stat. Sol. A **118**, 295 (1990)
18. J.P. Wang, Proc. IEEE **96**, 1847 (2008)
19. B. Stahl, J. Ellrich, R. Theissmann, M. Ghafari, S. Bhattacharya, H. Hahn, N.S. Gajghiye, D. Kramer, R.N. Viswanath, J. Weissmuller, H. Gleiter, Phys. Rev. B **67**, 14422 (2003)
20. T. Thomson, B.D. Terries, M.F. Toney, S. Raoux, J.E.E.E. Baglin, S.L. Lee, S. Sun, J. Appl. Phys. **95**, 6738 (2004)
21. S. Yamamoto, Y. Morimoto, T. Ono, M. Takano, Appl. Phys. Lett. **87**, 032503 (2005)
22. M. Suda, Y. Einaga, Angew. Chem. Int. Ed. **48**, 1754 (2009)
23. P. Rasmussen, X. Rui, J.E. Shield, Appl. Phys. Lett. **86**, 191915 (2005)
24. E.P. Wohlfarth, J. Appl. Phys. **29**, 595 (1958)
25. H. Zeng, S.H. Sun, T.S. Vedantam, J.P. Liu, Z.R. Dai, Z.L. Wang, Appl. Phys. Lett. **80**, 2583 (2002)